Constraints on holographic QCD phase transitions from PTA observations

Song He[1,6],* Li Li[2,3,5],† Sai Wang[4,5],‡ and Shao-Jiang Wang[2]§
[1] *Center for Theoretical Physics and College of Physics, Jilin University, Changchun 130012, China*
[2] *CAS Key Laboratory of Theoretical Physics, Institute of Theoretical Physics, Chinese Academy of Sciences, Beijing 100190, China*
[3] *School of Fundamental Physics and Mathematical Sciences, Hangzhou Institute for Advanced Study, UCAS, Hangzhou 310024, China*
[4] *Theoretical Physics Division, Institute of High Energy Physics, Chinese Academy of Sciences, Beijing 100049, China*
[5] *School of Physical Sciences, University of Chinese Academy of Sciences (UCAS), Beijing 100049, China and*
[6] *Max Planck Institute for Gravitational Physics (Albert Einstein Institute), Am Mühlenberg 1, 14476 Golm, Germany*

The underlying physics of QCD phase transition in the early Universe remains largely unknown due to its strong-coupling nature during the quark-gluon plasma/hadron gas transition, yet a holographic model has been proposed to quantitatively fit the lattice QCD data while with its duration of the first-order phase transition (FoPT) left undetermined. At specific baryon chemical potential, the first-order QCD phase transition agrees with the observational constraint of baryon asymmetry. It therefore provides a scenario for phase transition gravitational waves (GWs) within the Standard Model of particle physics. If these background GWs could contribute dominantly to the recently claimed common-spectrum red noise from pulsar timing array (PTA) observations, the duration of this FoPT can be well constrained but disfavored by the constraints from curvature perturbations. However, the associated primordial black holes are still allowed by current observations. Therefore, either the QCD phase transition is not described by our holographic model or the other GW sources must be presented to dominate over the GWs from this FoPT.

Introduction.— Recently, independent evidence for detecting a gravitational-wave (GW) background around the nano-Hz band has been reported by different observations using pulsar timing array (PTA) [1–4], among which the Chinese PTA Data Release I (CPTA DR1) [1] has found the highest statistical significance (4.6σ) for the Hellings–Downs correlation curve [5], while the North American Nanohertz Observatory for Gravitational Waves 15-year data (NANOGrav 15yr) [2] has put strong constraints on the excluded parameter spaces for various cosmological sources [6] (see also [7]) when their GWs significantly exceed the NANOGrav signal. Nevertheless, although the 10.3-year subset of European Pulsar Timing Array second data release (EPTA DR2) [3] based on modern observing systems renders a 15 times larger Bayes factor of GW background detection compared to that of the full 24.7-year EPTA data set, its inferred spectrum is in mild tension with the common signal measured in the full data set. Similarly, the first half of the Parkes Pulsar Timing Array third data release (PPTA DR3) [4] yields an upper limit on the inferred common-spectrum amplitude in tension with that from the complete data set.

However, if the signal is indeed genuine, we are in a position to search for other GW sources (for example, cosmic inflation [8–14], scalar-induced GWs [15–26], phase transitions [17, 27–42], domain walls [17, 38, 43–51], cosmic strings [17, 38, 52–57], and ultralight dark matter [58], to name just a few) in addition to the conventional background from inspiraling supermassive black hole binaries (SMBHBs), even though the SMBHB background itself might also call for better modeling from unknown environmental effects [59–65].

The cosmological quantum chromodynamics (QCD) phase transition holds significant implications as a potential source for a stochastic GW background if it is of the first order. However, constraints imposed by measurements of primordial element abundances and the cosmic microwave background have led to a stringent limitation on the baryon asymmetry $\eta_B \equiv n_B/s$, where n_B and s denote the baryon number density and entropy density, respectively [66]. The observed value [67], $\eta_B \approx 10^{-10}$, has led to the prevailing belief that a cosmological first-order QCD phase transition does not occur within the Standard Model of particle physics. Hence, numerous QCD model buildings beyond the Standard Model have been proposed to introduce a first-order phase transition (FoPT) (e.g., see specifically Refs. [68–76] and most recent review [77]).

While both experimental data and lattice QCD provide insights mainly within the crossover region with $\mu_B/T \leq 3.5$, we have leveraged holographic duality to establish a connection between the non-perturbative dynamics of QCD and a higher-dimensional gravity system. Our holographic model has not only demonstrated a remarkable quantitative agreement with state-of-the-art lattice QCD data for 2+1 flavors [78] (see also Refs. [79, 80] and particularly [81]), but it also has recently exhibited consistency with experimental data from heavy ion collisions regarding baryon number fluctuations along chemical freeze-out [82]. Notably, the critical endpoint (CEP) in the QCD phase diagram is located at ($T_{\rm CEP} = 105$ MeV, $\mu_{\rm CEP} = 555$ MeV), a region that is anticipated to be accessible to upcoming experimen-

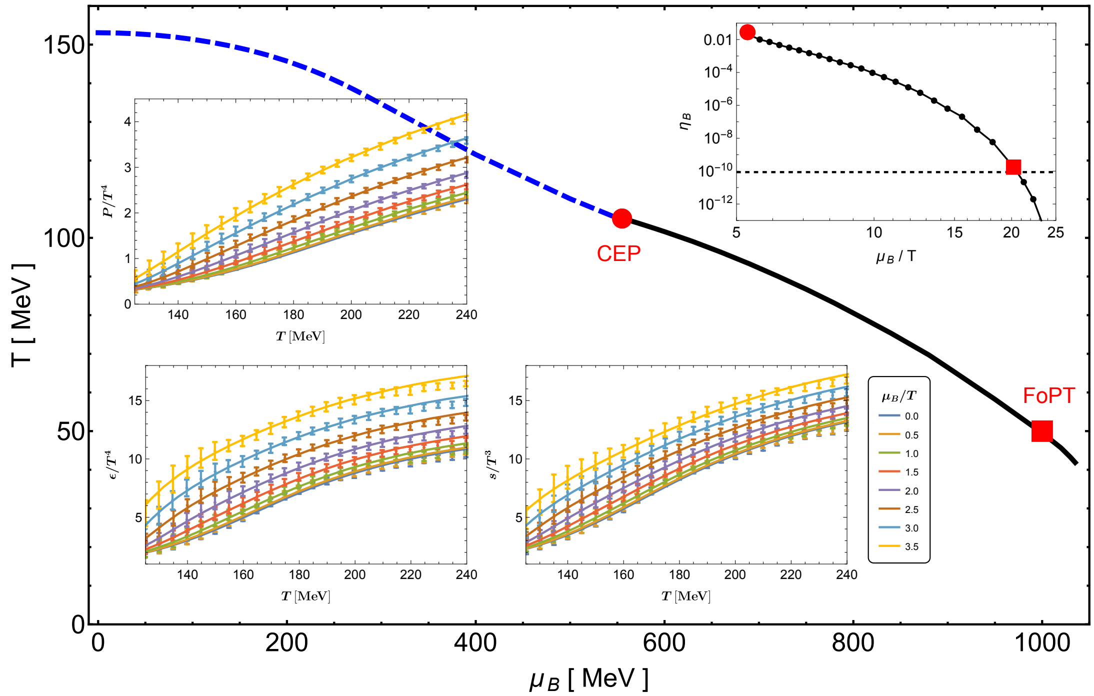

FIG. 1. Summary of our holographic model predictions. The QCD phase diagram is shown in the $T-\mu_B$ plane with the red point (CEP) separating the crossover (blue dashed) and first-order (black solid) regimes. The blue dashed line is determined by the maximally increasing point of the baryon number susceptibility and the black solid one is by the free energy. The bottom-left three insets present our holographic computations of pressure P, energy density ϵ, and entropy density s compared to the latest lattice data (with error bars) within the available range $0 < \mu_B/T < 3.5$, while the upper-right inset presents our model prediction on the baryon asymmetry with the red square singled out to match the observational value (dashed line).

tal measurements [78]. Intriguingly, our theory within the confines of the Standard Model finds that around $\mu_B = 1000$ MeV, not only does the QCD phase transition become first order, but also the inferred value of η_B aligns with cosmological observations. This presents a compelling scenario where the early universe, as described by the Standard Model, could have served as an essential source of GWs.

In this paper, we will use the NANOGrav 15yr data [2] to constrain the parameter space of the FoPT predicted by our holographic QCD model assuming that it produces the dominant contribution to the NANOGrav signals. In particular, the Bayes parameter inferences allow us to put a strong constraint on the duration of this FoPT, which is already disfavored by the constraints from curvature perturbations even though the produced primordial black holes (PBHs) are still allowed by current observations. This could either disfavor our scenario at the benchmark point with $\mu_B = 1000$ MeV as a viable description for a first-order QCD phase transition, or the QCD phase transition by itself does not contribute dominantly to the NANOGrav signals, and other GW sources must be present.

Holographic model.— The holographic model used to describe QCD with 2+1 flavors is represented by the following action [78]

$$S_M = \frac{1}{2\kappa_N^2}\int d^5x\sqrt{-g}[\mathcal{R}-\frac{1}{2}(\nabla\phi)^2-\frac{Z(\phi)}{4}F_{\mu\nu}F^{\mu\nu}-V(\phi)]\,, \tag{1}$$

where A_μ is the gauge field incorporating finite baryon density and ϕ accounts for the breaking of conformal invariance in the dual system. Alongside the effective Newton constant κ_N^2, $V(\phi)$ and $Z(\phi)$ are two independent couplings within our bottom-up model. The solution describing the hairy black hole configuration is given by

$$\begin{aligned} ds^2 &= -f(r)e^{-\eta(r)}dt^2 + \frac{dr^2}{f(r)} + r^2 d\boldsymbol{x}_3^2\,, \\ \phi &= \phi(r), \quad A_t = A_t(r)\,. \end{aligned} \tag{2}$$

In this context, $d\boldsymbol{x}_3^2 = dx^2 + dy^2 + dz^2$, and r denotes the radial coordinate in the holographic setup. The AdS boundary is located as $r \to \infty$. Thermodynamic quantities such as temperature T, entropy density s, energy density ϵ, and pressure P can be straightforwardly derived using the standard holographic dictionary.

To encapsulate non-perturbative effects and flavor dynamics, we have employed global fitting techniques to calibrate the model parameters with state-of-the-art lattice data for (2+1)-flavors at zero net-baryon density.

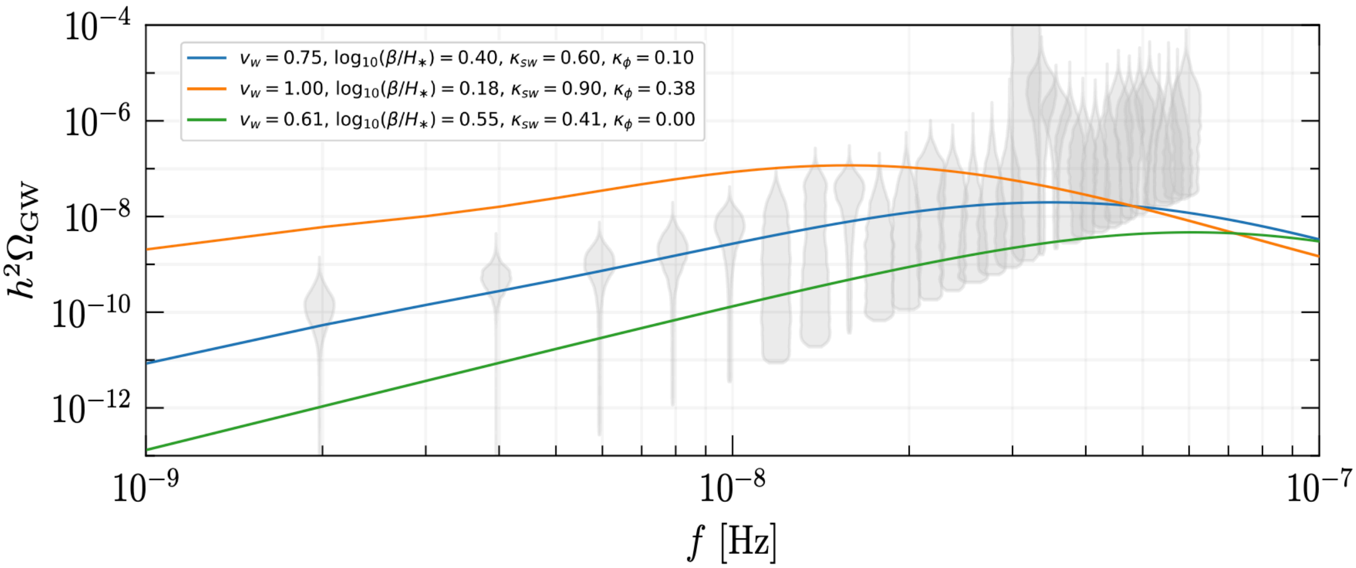

FIG. 2. Energy-density fraction spectra with three different sets of values for the four independent model parameters. Violin data points stand for the NANOGrav 15yr observations [2].

The explicit forms of $V(\phi)$ and $Z(\phi)$ are given by:

$$\begin{aligned} V(\phi) &= -12\cosh[c_1\phi] + (6c_1^2 - \frac{3}{2})\phi^2 + c_2\phi^6\,, \\ Z(\phi) &= \frac{1}{1+c_3}\mathrm{sech}[c_4\phi^3] + \frac{c_3}{1+c_3}e^{-c_5\phi}\,, \end{aligned} \tag{3}$$

with $c_1 = 0.7100, c_2 = 0.0037, c_3 = 1.935, c_4 = 0.085, c_5 = 30$. Moreover, $\kappa_N^2 = 2\pi(1.68)$ and the source of ϕ reads $\phi_s = r\phi|_{r\to\infty} = 1085$ MeV that essentially breaks the conformal symmetry and plays the role of the energy scale. Further details and explanations can be found in Ref. [78].

This comprehensive framework aligns theoretical predictions with the underlying physics of the QCD phase transition and yields insights into its thermodynamic properties as shown in the phase diagram of Fig. 1, where the bottom-left three insets present direction comparisons between our holographic computations on the pressure, energy density, and entropy density with respective to the latest lattice results [83] only available for $\mu_B/T \le 3.5$, while the upper-right inset presents our model prediction on the baryon asymmetry with the red square coincided with the observational value. In particular, our model predicts the phase transition between the color-neutral hadronic phase at low T and small μ_B and the quark-gluon plasma at high T and large μ_B. The transition is a smooth crossover at small μ_B and changes into a first-order one for higher μ_B. The critical point between them is at ($T_{\rm CEP} = 105$ MeV, $\mu_{\rm CEP} = 555$ MeV) which is denoted as the red point of Fig. 1. We are particularly interested in the first-order QCD phase transition at $\mu_B = 1000$ MeV (the red square of Fig. 1), which agrees with the observational constraint of a tiny baryon asymmetry, and thus provides a scenario for phase transition GWs within the Standard Model. For the FoPT at $\mu_B = 1000$ MeV, the critical temperature $T_* = 49.53$ MeV and the phase transition strength between the false (+) and true (−) vacuum reads

$$\alpha = \frac{\theta_+ - \theta_-}{3w_+}\Big|_{T=T_n} = \frac{\epsilon_+(T_n) - \epsilon_-(T_n)}{3w_+(T_n)} = 0.33\,, \tag{4}$$

with $\theta = \epsilon - 3P$ the trace anomaly and $w = \epsilon + P$ the enthalpy. The effective number of relativistic degrees of freedom $g_{\rm dof} = 45s_+/(2\pi^2 T_*^3) = 185$.

Gravitational waves.— As our holographic model predicts a FoPT around the temperature $T_* = 49.53$ MeV with a strength factor $\alpha = 0.33$ and the effective number of degrees of freedom $g_{\rm dof} = 185$, the parameter space for the produced GWs shrinks down to four parameters, namely, the effective duration β^{-1} of phase transition appeared in the combination β/H_* with H_* being the Hubble parameter at T_*, the terminal wall speed v_w of bubble expansion, the efficiency factor κ_ϕ of converting the released vacuum energy into the wall motion, and the efficiency factor $\kappa_{\rm sw}$ of converting the released vacuum energy into the fluid motions. The GW spectrum from bubble wall collisions is analytically captured by the envelope approximation with the fitting formula [84–86],

$$\begin{aligned} h^2\Omega_{\rm env} = 1.67\times10^{-5}\left(\frac{100}{g_{\rm dof}}\right)^{\frac{1}{3}}\left(\frac{H_*}{\beta}\right)^2\left(\frac{\kappa_\phi\alpha}{1+\alpha}\right)^2 \\ \times\frac{0.48v_w^3}{1+5.3v_w^2+5v_w^4}S_{\rm env}(f)\,, \end{aligned} \tag{5}$$

where the spectral shape is of a three-section form,

$$S_{\rm env}(f) = \frac{1}{c_l\left(\frac{f}{f_{\rm env}}\right)^{-3} + (1-c_l-c_h)\left(\frac{f}{f_{\rm env}}\right)^{-1} + c_h\left(\frac{f}{f_{\rm env}}\right)} \tag{6}$$

with $c_l = 0.064$ and $c_h = 0.48$, and the peak frequency is given by

$$f_{\rm env} = 1.65\times 10^{-5}\,{\rm Hz}\left(\frac{g_{\rm dof}}{100}\right)^{\frac{1}{6}}\left(\frac{T_*}{100\,{\rm GeV}}\right) \times \frac{0.35(\beta/H_*)}{1+0.069v_w+0.69v_w^4}\,. \tag{7}$$

The GW spectrum from fluid motions is dominated by sound waves [87–93] fitted by numerical simulations [87–89] as

$$h^2\Omega_{\rm sw} = 2.65\times 10^{-6}\left(\frac{100}{g_{\rm dof}}\right)^{\frac{1}{3}}\left(\frac{H_*}{\beta}\right)\left(\frac{\kappa_{\rm sw}\alpha}{1+\alpha}\right)^2 \times \frac{7^{7/2}v_w(f/f_{\rm sw})^3}{(4+3(f/f_{\rm sw})^2)^{7/2}}\Upsilon \tag{8}$$

with the peak frequency given by

$$f_{\rm sw} = 1.9\times 10^{-5}\,{\rm Hz}\left(\frac{g_{\rm dof}}{100}\right)^{\frac{1}{6}}\left(\frac{T_*}{100\,{\rm GeV}}\right)\left(\frac{1}{v_w}\right)\left(\frac{\beta}{H_*}\right)\,, \tag{9}$$

where the spectral shape at low frequencies can be analytically modeled [93] as forced collisions of sound shells during bubble percolations, while the spectral shape at high frequencies can be analytically modeled [90, 91] as free collisions of sound shells long after bubble percolations. Here, the suppression factor $\Upsilon \equiv 1-(1+2\tau_{\rm sw}H_*)^{-1/2}$ [92] accounts for the finite lifetime of sound waves from the onset timescale of turbulences, $\tau_{\rm sw}H_* \approx (8\pi)^{1/3}v_w/(\beta/H_*)/\bar{U}_f$ with the root-mean-squared fluid speed $\bar{U}_f^2 = 3\kappa_{\rm sw}\alpha/[4(1+\alpha)]$.

PTA constraints.— Our holographic model has already fixed three parameters $(T_*, \alpha, g_{\rm dof})$ but is left with four parameters $(\beta/H_*, v_w, \kappa_\phi, \kappa_{\rm sw})$, which are all independent parameters *in practice* as argued shortly below. For a bag equation of state (EoS), the efficiency factor $\kappa_{\rm sw}$ of fluid motions can be determined as a function [94] of the strength factor α and wall speed v_w, but it eventually becomes model-dependent when going beyond the bag EoS [95–99]. For our holographic model, the sound speeds in the false and true vacua can be calculated as $c_+^2 = 0.15$ and $c_-^2 = 0.14$, respectively, which deviate significantly from the bag EoS with the sound speed $c_s^2 = 1/3$. Hence, we will treat $\kappa_{\rm sw}$ as an independent parameter. The determination for the wall speed v_w is even more model-dependent [100–104] (see, however, the recent attempts of model-independent approaches [105, 106] from local equilibrium and strong coupling [107, 108], respectively), and hence the wall speed v_w is also treated as an independent parameter. As for the efficiency factor κ_ϕ of wall collisions, it always admits an extra dependence on the leading-order friction term [109–111] whenever the GWs are dominated by wall collisions or fluid motions [111, 112]. Therefore, κ_ϕ is also model-dependent and treated as an independent parameter as well. Last, β/H_* is an independent parameter of FoPT on its own (see, however, Ref. [113] from a holographic computation).

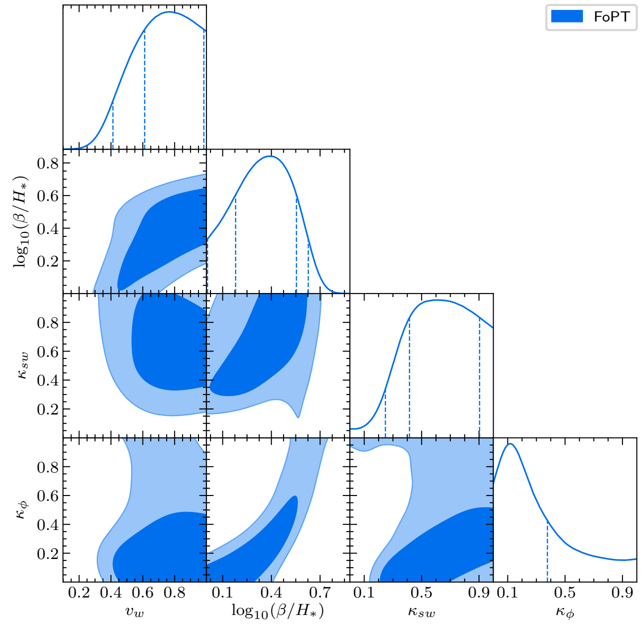

FIG. 3. Posteriors of the four independent model parameters inferred from the NANOGrav 15-year data release [2].

Following the approach of Ref. [6], we perform Bayes parameter inferences and obtain the parameter region allowed by the NANOGrav 15-year data [2]. We set flat priors for all the four independent model parameters in their allowing ranges within $\log_{10}(\beta/H_*) \in [0,3]$, $v_w \in [0,1]$, $\kappa_\phi \in [0,1]$, and $\kappa_{\rm sw} \in [0,1]$, respectively. Here, the upper bound for β/H_* is conservatively chosen with a large number. In Fig. 2, we depict the GW energy-density fraction spectra, given three different sets of values for these independent parameters. Performing Bayes analysis, we obtain the posteriors of these parameters that are shown in Fig. 3. Correspondingly, the median values and uncertainties of these parameters are inferred to be $\log_{10}(\beta/H_*) = 0.40^{+0.15}_{-0.23}$, $v_w = 0.76^{+0.22}_{-0.15}$, $\kappa_\phi = 0.12^{+0.26}_{-0.12}$, and $\kappa_{\rm sw} = 0.62^{+0.28}_{-0.20}$ at 68% confidence level. Furthermore, we plot the blue solid curve in Fig. 2 from the peak value of one-dimensional posterior for each parameter after marginalized over all the other parameters as shown in Fig. 3. The curve seems to be capable of fitting nicely with the NANOGrav 15yr data.

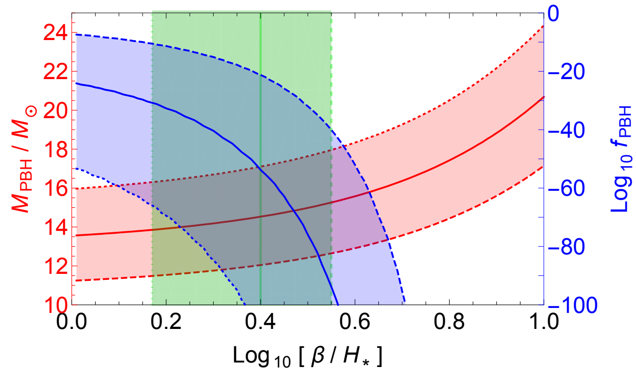

FIG. 4. The constraints on the PBH mass (red) and abundance (blue) from the delayed decay mechanism given the PTA constraints on $\log_{10}(\beta/H_*)$ (green) and v_w, where the dotted and dashed curves are obtained from the corresponding 1σ lower and upper bounds of v_w, respectively.

Other constraints.— As a general property of any FoPT, the vacuum decay process is not simultaneous all over the space, and hence there is always a non-vanishing chance to find Hubble-scale regions where the vacuum decay progress falls behind their ambient regions [114]. Since the false vacuum energy can never be diluted away while the radiations would with the Hubble expansion of our Universe, the total energy density in these delayed-decay regions would gradually accumulate their density contrasts to enhance the curvature perturbations [115] or even form PBHs [116] when exceeding the PBH threshold. See also Refs. [117, 118] for recent improved treatments on Refs. [119, 120]. Therefore, there are always accompanying constraints other than GWs from PBHs and curvature perturbations. Following the same procedure of Ref. [116] (see also Ref. [79]), we can calculate the associated PBH formations as shown in Fig. 4, where the PBH mass (red) and abundance (blue) are obtained for given β/H_* and v_w with their 1σ uncertainties expanded between the dotted (lower bound) and dashed (upper bound) lines. All the other parameters are fixed by our holographic model. In particular, the sound speed $c_+^2 = 0.15$ in the false vacuum analytically fixes the PBH threshold $\delta_c = [3(1+w)/(5+3w)]\sin^2[\pi\sqrt{w}/(1+3w)] = 0.35$ [121]. It is easy to see that the produced PBH mass is roughly between $\sim 11-18\,M_\odot$ and the PBH abundance $f_{\rm PBH} \lesssim 10^{-10}$ is so tiny that the current observational constraint [122] in this mass range can still be evaded.

However, this is not the case for the constraints from curvature perturbations based on the recent scenario [115], where the low-scale phase transition with this large $\alpha = 0.3$ and small $\beta/H_* \sim 1.5 - 3.5$ would already be disfavoured by the constraints from the ultracompact minihalo abundance [123, 124]. Note that a small β/H_* is also argued to be disfavored from holographic side but at the probe limit [125]. Therefore, at least our holographic model at the benchmark point with $\mu_B = 1000$ MeV seems not to be favored by the current observations, while other chemical potential would require a little inflation [68, 69] during the QCD phase transition to achieve the observed baryon asymmetry, which will be reserved for future study.

Conclusions and discussions.— The cosmological QCD phase transition is still a myth to both communities from particle physics and nuclear physics, and whether it is of the first order can be tested by stochastic GW backgrounds possibly detectable from PTA observations. Recent observations of a low-frequency GW background from NANOGrav, EPTA, PPTA, and CPTA provide a promising opportunity to test various first-order QCD phase transition models, in particular, our holographic model aligned quantitatively with lattice QCD data, which is strongly constrained by the NANOGrav 15yr data, especially for its phase-transition duration parameter. All these constraints along with the parameters fixed already by the holographic model can be transformed into constraints on the associated PBH formations by the delayed decay mechanism. Although the produced PBH abundance is still observationally allowed, the induced curvature perturbations are too large to meet current constraints from the ultracompact minihalo abundance.

Several possibilities can be inferred from above results: (i) the strongest claim we can make is that perhaps the QCD phase transition is actually a smooth crossover without the associated GW background at all; (ii) the QCD phase transition is indeed of first order but is not described by our holographic model; (iii) the QCD phase transition is indeed of first order and it is also described by our model but at a different chemical potential with extra assistance from a little inflation during the phase transition; (iv) the weakest claim is simply that the QCD phase transition is indeed described by our holographic model at $\mu_B = 1000$ MeV but other GW sources dominate over the GW background from this FoPT.

We thank Rong-Gen Cai, Qing-Xuan Fu, Yuan-Xu Wang, Hong-An Zeng, and Zhi-Chao Zhao for the valuable discussions. This work is supported by the National Key Research and Development Program of China Grant No. 2021YFC2203004, No. 2021YFA0718304, and No. 2020YFC2201501, the National Natural Science Foundation of China Grants No. 12075101, No. 12235016, No. 12175243, No. 12105344, No. 12122513, No. 12075298, No. 11991052, No. 12235019, and No. 12047503, the Fundamental Research Funds for the Central Universities, the Max Planck Partner group research grant, the Chinese Academy of Sciences Project for Young Scientists in Basic Research YSBR-006, and the Science Research Grants from the China Manned Space Project with No. CMS-CSST-2021-B01.

* hesong@jlu.edu.cn
† liliphy@itp.ac.cn
‡ wangsai@ihep.ac.cn
§ schwang@itp.ac.cn

[1] H. Xu et al., "Searching for the Nano-Hertz Stochastic Gravitational Wave Background with the Chinese Pulsar Timing Array Data Release I," Res. Astron. Astrophys. **23** no. 7, (2023) 075024, arXiv:2306.16216 [astro-ph.HE].
[2] **NANOGrav** Collaboration, G. Agazie et al., "The NANOGrav 15 yr Data Set: Evidence for a Gravitational-wave Background," Astrophys. J. Lett. **951** no. 1, (2023) L8, arXiv:2306.16213 [astro-ph.HE].
[3] J. Antoniadis et al., "The second data release from the European Pulsar Timing Array I. The dataset and timing analysis," arXiv:2306.16224 [astro-ph.HE].
[4] D. J. Reardon et al., "Search for an Isotropic Gravitational-wave Background with the Parkes Pulsar Timing Array," Astrophys. J. Lett. **951** no. 1, (2023) L6, arXiv:2306.16215 [astro-ph.HE].
[5] R. w. Hellings and G. s. Downs, "UPPER LIMITS ON THE ISOTROPIC GRAVITATIONAL RADIATION BACKGROUND FROM PULSAR TIMING ANALYSIS," Astrophys. J. Lett. **265** (1983) L39–L42.
[6] **NANOGrav** Collaboration, A. Afzal et al., "The NANOGrav 15 yr Data Set: Search for Signals from New Physics," Astrophys. J. Lett. **951** no. 1, (2023) L11, arXiv:2306.16219 [astro-ph.HE].
[7] E. Madge, E. Morgante, C. Puchades-Ibáñez, N. Ramberg, W. Ratzinger, S. Schenk, and P. Schwaller, "Primordial gravitational waves in the nano-Hertz regime and PTA data – towards solving the GW inverse problem," arXiv:2306.14856 [hep-ph].
[8] S. Vagnozzi, "Inflationary interpretation of the stochastic gravitational wave background signal detected by pulsar timing array experiments," JHEAp **39** (2023) 81–98, arXiv:2306.16912 [astro-ph.CO].
[9] D. Borah, S. Jyoti Das, and R. Samanta, "Inflationary origin of gravitational waves with \textitMiracle-less WIMP dark matter in the light of recent PTA results," arXiv:2307.00537 [hep-ph].
[10] S. Datta, "Inflationary gravitational waves, pulsar timing data and low-scale-leptogenesis," arXiv:2307.00646 [hep-ph].
[11] X. Niu and M. H. Rahat, "NANOGrav signal from axion inflation," arXiv:2307.01192 [hep-ph].
[12] S. Choudhury, "Single field inflation in the light of NANOGrav 15-year Data: Quintessential interpretation of blue tilted tensor spectrum through Non-Bunch Davies initial condition," arXiv:2307.03249 [astro-ph.CO].
[13] J.-Q. Jiang, Y. Cai, G. Ye, and Y.-S. Piao, "Broken blue-tilted inflationary gravitational waves: a joint analysis of NANOGrav 15-year and BICEP/Keck 2018 data," arXiv:2307.15547 [astro-ph.CO].
[14] I. Ben-Dayan, U. Kumar, U. Thattarampilly, and A. Verma, "Probing The Early Universe Cosmology With NANOGrav: Possibilities and Limitations," arXiv:2307.15123 [astro-ph.CO].
[15] S. Wang, Z.-C. Zhao, J.-P. Li, and Q.-H. Zhu, "Exploring the Implications of 2023 Pulsar Timing Array Datasets for Scalar-Induced Gravitational Waves and Primordial Black Holes," arXiv:2307.00572 [astro-ph.CO].
[16] G. Franciolini, A. Iovino, Junior., V. Vaskonen, and H. Veermae, "The recent gravitational wave observation by pulsar timing arrays and primordial black holes: the importance of non-gaussianities," arXiv:2306.17149 [astro-ph.CO].
[17] L. Bian, S. Ge, J. Shu, B. Wang, X.-Y. Yang, and J. Zong, "Gravitational wave sources for Pulsar Timing Arrays," arXiv:2307.02376 [astro-ph.HE].
[18] K. Inomata, K. Kohri, and T. Terada, "The Detected Stochastic Gravitational Waves and Subsolar-Mass Primordial Black Holes," arXiv:2306.17834 [astro-ph.CO].
[19] S. A. Hosseini Mansoori, F. Felegray, A. Talebian, and M. Sami, "PBHs and GWs from $\mathbb{T}^2$-inflation and NANOGrav 15-year data," JCAP **08** (2023) 067, arXiv:2307.06757 [astro-ph.CO].
[20] L. Liu, Z.-C. Chen, and Q.-G. Huang, "Implications for the non-Gaussianity of curvature perturbation from pulsar timing arrays," arXiv:2307.01102 [astro-ph.CO].
[21] K. T. Abe and Y. Tada, "Translating nano-Hertz gravitational wave background into primordial perturbations taking account of the cosmological QCD phase transition," arXiv:2307.01653 [astro-ph.CO].
[22] J.-H. Jin, Z.-C. Chen, Z. Yi, Z.-Q. You, L. Liu, and Y. Wu, "Confronting sound speed resonance with pulsar timing arrays," arXiv:2307.08687 [astro-ph.CO].
[23] Q.-H. Zhu, Z.-C. Zhao, and S. Wang, "Joint implications of BBN, CMB, and PTA Datasets for Scalar-Induced Gravitational Waves of Second and Third orders," arXiv:2307.03095 [astro-ph.CO].
[24] S. Balaji, G. Domènech, and G. Franciolini, "Scalar-induced gravitational wave interpretation of PTA data: the role of scalar fluctuation propagation speed," arXiv:2307.08552 [gr-qc].
[25] Z.-C. Zhao, Q.-H. Zhu, S. Wang, and X. Zhang, "Exploring the Equation of State of the Early Universe: Insights from BBN, CMB, and PTA Observations," arXiv:2307.13574 [astro-ph.CO].
[26] L. Liu, Z.-C. Chen, and Q.-G. Huang, "Probing the equation of state of the early Universe with pulsar timing arrays," arXiv:2307.14911 [astro-ph.CO].
[27] A. Addazi, Y.-F. Cai, A. Marciano, and L. Visinelli, "Have pulsar timing array methods detected a cosmological phase transition?," arXiv:2306.17205 [astro-ph.CO].
[28] P. Athron, A. Fowlie, C.-T. Lu, L. Morris, L. Wu, Y. Wu, and Z. Xu, "Can supercooled phase transitions explain the gravitational wave background observed by pulsar timing arrays?," arXiv:2306.17239 [hep-ph].
[29] K. Fujikura, S. Girmohanta, Y. Nakai, and M. Suzuki, "NANOGrav Signal from a Dark Conformal Phase Transition," arXiv:2306.17086 [hep-ph].
[30] C. Han, K.-P. Xie, J. M. Yang, and M. Zhang, "Self-interacting dark matter implied by nano-Hertz gravitational waves," arXiv:2306.16966 [hep-ph].
[31] G. Franciolini, D. Racco, and F. Rompineve, "Footprints of the QCD Crossover on Cosmological Gravitational Waves at Pulsar Timing Arrays,"

arXiv:2306.17136 [astro-ph.CO].
[32] S. Jiang, A. Yang, J. Ma, and F. P. Huang, "Implication of nano-Hertz stochastic gravitational wave on dynamical dark matter through a first-order phase transition," arXiv:2306.17827 [hep-ph].
[33] T. Ghosh, A. Ghoshal, H.-K. Guo, F. Hajkarim, S. F. King, K. Sinha, X. Wang, and G. White, "Did we hear the sound of the Universe boiling? Analysis using the full fluid velocity profiles and NANOGrav 15-year data," arXiv:2307.02259 [astro-ph.HE].
[34] Y. Xiao, J. M. Yang, and Y. Zhang, "Implications of Nano-Hertz Gravitational Waves on Electroweak Phase Transition in the Singlet Dark Matter Model," arXiv:2307.01072 [hep-ph].
[35] S.-P. Li and K.-P. Xie, "A collider test of nano-Hertz gravitational waves from pulsar timing arrays," arXiv:2307.01086 [hep-ph].
[36] P. Di Bari and M. H. Rahat, "The split majoron model confronts the NANOGrav signal," arXiv:2307.03184 [hep-ph].
[37] J. S. Cruz, F. Niedermann, and M. S. Sloth, "NANOGrav meets Hot New Early Dark Energy and the origin of neutrino mass," arXiv:2307.03091 [astro-ph.CO].
[38] Y.-M. Wu, Z.-C. Chen, and Q.-G. Huang, "Cosmological Interpretation for the Stochastic Signal in Pulsar Timing Arrays," arXiv:2307.03141 [astro-ph.CO].
[39] X. K. Du, M. X. Huang, F. Wang, and Y. K. Zhang, "Did the nHZ Gravitational Waves Signatures Observed By NANOGrav Indicate Multiple Sector SUSY Breaking?," arXiv:2307.02938 [hep-ph].
[40] Y. Gouttenoire, "First-order Phase Transition interpretation of PTA signal produces solar-mass Black Holes," arXiv:2307.04239 [hep-ph].
[41] M. Ahmadvand, L. Bian, and S. Shakeri, "A Heavy QCD Axion model in Light of Pulsar Timing Arrays," arXiv:2307.12385 [hep-ph].
[42] D. Wang, "Constraining Cosmological Phase Transitions with Chinese Pulsar Timing Array Data Release 1," arXiv:2307.15970 [astro-ph.CO].
[43] Y. Bai, T.-K. Chen, and M. Korwar, "QCD-Collapsed Domain Walls: QCD Phase Transition and Gravitational Wave Spectroscopy," arXiv:2306.17160 [hep-ph].
[44] N. Kitajima, J. Lee, K. Murai, F. Takahashi, and W. Yin, "Nanohertz Gravitational Waves from Axion Domain Walls Coupled to QCD," arXiv:2306.17146 [hep-ph].
[45] S. Blasi, A. Mariotti, A. Rase, and A. Sevrin, "Axionic domain walls at Pulsar Timing Arrays: QCD bias and particle friction," arXiv:2306.17830 [hep-ph].
[46] Y. Gouttenoire and E. Vitagliano, "Domain wall interpretation of the PTA signal confronting black hole overproduction," arXiv:2306.17841 [gr-qc].
[47] B. Barman, D. Borah, S. Jyoti Das, and I. Saha, "Scale of Dirac leptogenesis and left-right symmetry in the light of recent PTA results," arXiv:2307.00656 [hep-ph].
[48] B.-Q. Lu and C.-W. Chiang, "Nano-Hertz stochastic gravitational wave background from domain wall annihilation," arXiv:2307.00746 [hep-ph].
[49] E. Babichev, D. Gorbunov, S. Ramazanov, R. Samanta, and A. Vikman, "NANOGrav spectral index $\gamma = 3$ from melting domain walls," arXiv:2307.04582 [hep-ph].
[50] Z. Zhang, C. Cai, Y.-H. Su, S. Wang, Z.-H. Yu, and H.-H. Zhang, "Nano-Hertz gravitational waves from collapsing domain walls associated with freeze-in dark matter in light of pulsar timing array observations," arXiv:2307.11495 [hep-ph].
[51] S. Ge, "Stochastic gravitational wave background: birth from axionic string-wall death," arXiv:2307.08185 [gr-qc].
[52] J. Ellis, M. Lewicki, C. Lin, and V. Vaskonen, "Cosmic Superstrings Revisited in Light of NANOGrav 15-Year Data," arXiv:2306.17147 [astro-ph.CO].
[53] Z. Wang, L. Lei, H. Jiao, L. Feng, and Y.-Z. Fan, "The nanohertz stochastic gravitational-wave background from cosmic string Loops and the abundant high redshift massive galaxies," arXiv:2306.17150 [astro-ph.HE].
[54] G. Lazarides, R. Maji, and Q. Shafi, "Superheavy quasi-stable strings and walls bounded by strings in the light of NANOGrav 15 year data," arXiv:2306.17788 [hep-ph].
[55] G. Servant and P. Simakachorn, "Constraining Post-Inflationary Axions with Pulsar Timing Arrays," arXiv:2307.03121 [hep-ph].
[56] S. Antusch, K. Hinze, S. Saad, and J. Steiner, "Singling out SO(10) GUT models using recent PTA results," arXiv:2307.04595 [hep-ph].
[57] M. Yamada and K. Yonekura, "Dark baryon from pure Yang-Mills theory and its GW signature from cosmic strings," arXiv:2307.06586 [hep-ph].
[58] M. Aghaie, G. Armando, A. Dondarini, and P. Panci, "Bounds on Ultralight Dark Matter from NANOGrav," arXiv:2308.04590 [astro-ph.CO].
[59] **NANOGrav** Collaboration, G. Agazie et al., "The NANOGrav 15 yr Data Set: Constraints on Supermassive Black Hole Binaries from the Gravitational-wave Background," Astrophys. J. Lett. **952** no. 2, (2023) L37, arXiv:2306.16220 [astro-ph.HE].
[60] J. Ellis, M. Fairbairn, G. Hütsi, J. Raidal, J. Urrutia, V. Vaskonen, and H. Veermäe, "Gravitational Waves from SMBH Binaries in Light of the NANOGrav 15-Year Data," arXiv:2306.17021 [astro-ph.CO].
[61] Z.-Q. Shen, G.-W. Yuan, Y.-Y. Wang, and Y.-Z. Wang, "Dark Matter Spike surrounding Supermassive Black Holes Binary and the nanohertz Stochastic Gravitational Wave Background," arXiv:2306.17143 [astro-ph.HE].
[62] Y.-C. Bi, Y.-M. Wu, Z.-C. Chen, and Q.-G. Huang, "Implications for the Supermassive Black Hole Binaries from the NANOGrav 15-year Data Set," arXiv:2307.00722 [astro-ph.CO].
[63] A. Ghoshal and A. Strumia, "Probing the Dark Matter density with gravitational waves from super-massive binary black holes," arXiv:2306.17158 [astro-ph.CO].
[64] P. F. Depta, K. Schmidt-Hoberg, and C. Tasillo, "Do pulsar timing arrays observe merging primordial black holes?," arXiv:2306.17836 [astro-ph.CO].
[65] Y. Gouttenoire, S. Trifinopoulos, G. Valogiannis, and M. Vanvlasselaer, "Scrutinizing the Primordial Black Holes Interpretation of PTA Gravitational Waves and JWST Early Galaxies," arXiv:2307.01457

[astro-ph.CO].

[66] S. Dodelson, Modern Cosmology. Elsevier Science, 2003. https://books.google.co.jp/books?id=3oPRxdXJexcC.

[67] B. D. Fields, K. A. Olive, T.-H. Yeh, and C. Young, "Big-Bang Nucleosynthesis after Planck," JCAP **03** (2020) 010, arXiv:1912.01132 [astro-ph.CO]. [Erratum: JCAP 11, E02 (2020)].

[68] T. Boeckel and J. Schaffner-Bielich, "A little inflation in the early universe at the QCD phase transition," Phys. Rev. Lett. **105** (2010) 041301, arXiv:0906.4520 [astro-ph.CO]. [Erratum: Phys. Rev. Lett.106,069901(2011)].

[69] T. Boeckel and J. Schaffner-Bielich, "A little inflation at the cosmological QCD phase transition," Phys. Rev. **D85** (2012) 103506, arXiv:1105.0832 [astro-ph.CO].

[70] P. Schwaller, "Gravitational Waves from a Dark Phase Transition," Phys. Rev. Lett. **115** no. 18, (2015) 181101, arXiv:1504.07263 [hep-ph].

[71] M. Aoki, H. Goto, and J. Kubo, "Gravitational Waves from Hidden QCD Phase Transition," Phys. Rev. **D96** no. 7, (2017) 075045, arXiv:1709.07572 [hep-ph].

[72] S. Iso, P. D. Serpico, and K. Shimada, "QCD-Electroweak First-Order Phase Transition in a Supercooled Universe," Phys. Rev. Lett. **119** no. 14, (2017) 141301, arXiv:1704.04955 [hep-ph].

[73] Y. Bai, A. J. Long, and S. Lu, "Dark Quark Nuggets," Phys. Rev. D **99** no. 5, (2019) 055047, arXiv:1810.04360 [hep-ph].

[74] P. Lu, V. Takhistov, and G. M. Fuller, "Signatures of a High Temperature QCD Transition in the Early Universe," Phys. Rev. Lett. **130** no. 22, (2023) 221002, arXiv:2212.00156 [astro-ph.CO].

[75] L. Sagunski, P. Schicho, and D. Schmitt, "Supercool exit: Gravitational waves from QCD-triggered conformal symmetry breaking," Phys. Rev. D **107** no. 12, (2023) 123512, arXiv:2303.02450 [hep-ph].

[76] A. Salvio, "Supercooling in Radiative Symmetry Breaking: Theory Extensions, Gravitational Wave Detection and Primordial Black Holes," arXiv:2307.04694 [hep-ph].

[77] P. Athron, C. Balázs, A. Fowlie, L. Morris, and L. Wu, "Cosmological phase transitions: from perturbative particle physics to gravitational waves," arXiv:2305.02357 [hep-ph].

[78] R.-G. Cai, S. He, L. Li, and Y.-X. Wang, "Probing QCD critical point and induced gravitational wave by black hole physics," Phys. Rev. D **106** no. 12, (2022) L121902, arXiv:2201.02004 [hep-th].

[79] S. He, L. Li, Z. Li, and S.-J. Wang, "Gravitational Waves and Primordial Black Hole Productions from Gluodynamics," arXiv:2210.14094 [hep-ph].

[80] Y.-Q. Zhao, S. He, D. Hou, L. Li, and Z. Li, "Phase diagram of holographic thermal dense QCD matter with rotation," JHEP **04** (2023) 115, arXiv:2212.14662 [hep-ph].

[81] E. Morgante, N. Ramberg, and P. Schwaller, "Gravitational waves from dark SU(3) Yang-Mills theory," Phys. Rev. D **107** no. 3, (2023) 036010, arXiv:2210.11821 [hep-ph].

[82] Z. Li, J. Liang, S. He, and L. Li, "Holographic study of higher-order baryon number susceptibilities at finite temperature and density," arXiv:2305.13874 [hep-ph].

[83] S. Borsányi, Z. Fodor, J. N. Guenther, R. Kara, S. D. Katz, P. Parotto, A. Pásztor, C. Ratti, and K. K. Szabó, "Lattice QCD equation of state at finite chemical potential from an alternative expansion scheme," Phys. Rev. Lett. **126** no. 23, (2021) 232001, arXiv:2102.06660 [hep-lat].

[84] D. J. Weir, "Gravitational waves from a first order electroweak phase transition: a brief review," Phil. Trans. Roy. Soc. Lond. **A376** no. 2114, (2018) 20170126, arXiv:1705.01783 [hep-ph].

[85] R. Jinno and M. Takimoto, "Gravitational waves from bubble collisions: An analytic derivation," Phys. Rev. **D95** no. 2, (2017) 024009, arXiv:1605.01403 [astro-ph.CO].

[86] S. J. Huber and T. Konstandin, "Gravitational Wave Production by Collisions: More Bubbles," JCAP **0809** (2008) 022, arXiv:0806.1828 [hep-ph].

[87] M. Hindmarsh, S. J. Huber, K. Rummukainen, and D. J. Weir, "Gravitational waves from the sound of a first order phase transition," Phys. Rev. Lett. **112** (2014) 041301, arXiv:1304.2433 [hep-ph].

[88] M. Hindmarsh, S. J. Huber, K. Rummukainen, and D. J. Weir, "Numerical simulations of acoustically generated gravitational waves at a first order phase transition," Phys. Rev. **D92** no. 12, (2015) 123009, arXiv:1504.03291 [astro-ph.CO].

[89] M. Hindmarsh, S. J. Huber, K. Rummukainen, and D. J. Weir, "Shape of the acoustic gravitational wave power spectrum from a first order phase transition," Phys. Rev. **D96** no. 10, (2017) 103520, arXiv:1704.05871 [astro-ph.CO]. [erratum: Phys. Rev.D101,no.8,089902(2020)].

[90] M. Hindmarsh, "Sound shell model for acoustic gravitational wave production at a first-order phase transition in the early Universe," Phys. Rev. Lett. **120** no. 7, (2018) 071301, arXiv:1608.04735 [astro-ph.CO].

[91] M. Hindmarsh and M. Hijazi, "Gravitational waves from first order cosmological phase transitions in the Sound Shell Model," JCAP **1912** (2019) 062, arXiv:1909.10040 [astro-ph.CO].

[92] H.-K. Guo, K. Sinha, D. Vagie, and G. White, "Phase Transitions in an Expanding Universe: Stochastic Gravitational Waves in Standard and Non-Standard Histories," JCAP **01** (2021) 001, arXiv:2007.08537 [hep-ph].

[93] R.-G. Cai, S.-J. Wang, and Z.-Y. Yuwen, "Hydrodynamic sound shell model," Phys. Rev. D **108** no. 2, (2023) L021502, arXiv:2305.00074 [gr-qc].

[94] J. R. Espinosa, T. Konstandin, J. M. No, and G. Servant, "Energy Budget of Cosmological First-order Phase Transitions," JCAP **1006** (2010) 028, arXiv:1004.4187 [hep-ph].

[95] F. Giese, T. Konstandin, K. Schmitz, and J. van de Vis, "Model-independent energy budget for LISA," JCAP **01** (2021) 072, arXiv:2010.09744 [astro-ph.CO].

[96] F. Giese, T. Konstandin, and J. van de Vis, "Model-independent energy budget of cosmological first-order phase transitions—A sound argument to go beyond the bag model," JCAP **2007** no. 07, (2020) 057, arXiv:2004.06995 [astro-ph.CO].

[97] X. Wang, F. P. Huang, and X. Zhang, "Energy budget and the gravitational wave spectra beyond the bag

model," Phys. Rev. D **103** no. 10, (2021) 103520, arXiv:2010.13770 [astro-ph.CO].

[98] S.-J. Wang and Z.-Y. Yuwen, "The energy budget of cosmological first-order phase transitions beyond the bag equation of state," JCAP **10** (2022) 047, arXiv:2206.01148 [hep-ph].

[99] X. Wang, C. Tian, and F. P. Huang, "Model-dependent analysis method for energy budget of the cosmological first-order phase transition," arXiv:2301.12328 [hep-ph].

[100] G. D. Moore and T. Prokopec, "Bubble wall velocity in a first order electroweak phase transition," Phys. Rev. Lett. **75** (1995) 777–780, arXiv:hep-ph/9503296 [hep-ph].

[101] G. D. Moore and T. Prokopec, "How fast can the wall move? A Study of the electroweak phase transition dynamics," Phys. Rev. **D52** (1995) 7182–7204, arXiv:hep-ph/9506475 [hep-ph].

[102] T. Konstandin, G. Nardini, and I. Rues, "From Boltzmann equations to steady wall velocities," JCAP **1409** (2014) 028, arXiv:1407.3132 [hep-ph].

[103] B. Laurent and J. M. Cline, "Fluid equations for fast-moving electroweak bubble walls," Phys. Rev. **D102** no. 6, (2020) 063516, arXiv:2007.10935 [hep-ph].

[104] B. Laurent and J. M. Cline, "First principles determination of bubble wall velocity," Phys. Rev. D **106** no. 2, (2022) 023501, arXiv:2204.13120 [hep-ph].

[105] W.-Y. Ai, B. Garbrecht, and C. Tamarit, "Bubble wall velocities in local equilibrium," JCAP **03** no. 03, (2022) 015, arXiv:2109.13710 [hep-ph].

[106] L. Li, S.-J. Wang, and Z.-Y. Yuwen, "Bubble expansion at strong coupling," arXiv:2302.10042 [hep-th].

[107] Y. Bea, J. Casalderrey-Solana, T. Giannakopoulos, D. Mateos, M. Sanchez-Garitaonandia, and M. Zilhão, "Bubble wall velocity from holography," Phys. Rev. D **104** no. 12, (2021) L121903, arXiv:2104.05708 [hep-th].

[108] R. A. Janik, M. Jarvinen, and J. Sonnenschein, "A simple description of holographic domain walls in confining theories — extended hydrodynamics," JHEP **09** (2021) 129, arXiv:2106.02642 [hep-th].

[109] J. Ellis, M. Lewicki, J. M. No, and V. Vaskonen, "Gravitational wave energy budget in strongly supercooled phase transitions," JCAP **1906** (2019) 024, arXiv:1903.09642 [hep-ph].

[110] J. Ellis, M. Lewicki, and V. Vaskonen, "Updated predictions for gravitational waves produced in a strongly supercooled phase transition," JCAP **2011** (2020) 020, arXiv:2007.15586 [astro-ph.CO].

[111] R.-G. Cai and S.-J. Wang, "Effective picture of bubble expansion," JCAP **2021** (2021) 096, arXiv:2011.11451 [astro-ph.CO].

[112] M. Lewicki and V. Vaskonen, "Gravitational waves from bubble collisions and fluid motion in strongly supercooled phase transitions," Eur. Phys. J. C **83** no. 2, (2023) 109, arXiv:2208.11697 [astro-ph.CO].

[113] F. R. Ares, O. Henriksson, M. Hindmarsh, C. Hoyos, and N. Jokela, "Gravitational Waves at Strong Coupling from an Effective Action," Phys. Rev. Lett. **128** no. 13, (2022) 131101, arXiv:2110.14442 [hep-th].

[114] A. H. Guth and E. J. Weinberg, "Could the Universe Have Recovered from a Slow First Order Phase Transition?," Nucl. Phys. B **212** (1983) 321–364.

[115] J. Liu, L. Bian, R.-G. Cai, Z.-K. Guo, and S.-J. Wang, "Constraining First-Order Phase Transitions with Curvature Perturbations," Phys. Rev. Lett. **130** no. 5, (2023) 051001, arXiv:2208.14086 [astro-ph.CO].

[116] J. Liu, L. Bian, R.-G. Cai, Z.-K. Guo, and S.-J. Wang, "Primordial black hole production during first-order phase transitions," Phys. Rev. D **105** no. 2, (2022) L021303, arXiv:2106.05637 [astro-ph.CO].

[117] Y. Gouttenoire and T. Volansky, "Primordial Black Holes from Supercooled Phase Transitions," arXiv:2305.04942 [hep-ph].

[118] I. Baldes and M. O. Olea-Romacho, "Primordial black holes as dark matter: Interferometric tests of phase transition origin," arXiv:2307.11639 [hep-ph].

[119] M. Lewicki, P. Toczek, and V. Vaskonen, "Primordial black holes from strong first-order phase transitions," arXiv:2305.04924 [astro-ph.CO].

[120] H. Kodama, M. Sasaki, and K. Sato, "Abundance of Primordial Holes Produced by Cosmological First Order Phase Transition," Prog. Theor. Phys. **68** (1982) 1979.

[121] T. Harada, C.-M. Yoo, and K. Kohri, "Threshold of primordial black hole formation," Phys. Rev. D **88** no. 8, (2013) 084051, arXiv:1309.4201 [astro-ph.CO]. [Erratum: Phys.Rev.D 89, 029903 (2014)].

[122] Z.-C. Chen, C. Yuan, and Q.-G. Huang, "Confronting the primordial black hole scenario with the gravitational-wave events detected by LIGO-Virgo," Phys. Lett. B **829** (2022) 137040, arXiv:2108.11740 [astro-ph.CO].

[123] H. A. Clark, G. F. Lewis, and P. Scott, "Investigating dark matter substructure with pulsar timing – I. Constraints on ultracompact minihaloes," Mon. Not. Roy. Astron. Soc. **456** no. 2, (2016) 1394–1401, arXiv:1509.02938 [astro-ph.CO]. [Erratum: Mon.Not.Roy.Astron.Soc. 464, 2468 (2017)].

[124] H. A. Clark, G. F. Lewis, and P. Scott, "Investigating dark matter substructure with pulsar timing – II. Improved limits on small-scale cosmology," Mon. Not. Roy. Astron. Soc. **456** no. 2, (2016) 1402–1409, arXiv:1509.02941 [astro-ph.CO]. [Erratum: Mon.Not.Roy.Astron.Soc. 464, 955–956 (2017)].

[125] Y. Chen, D. Li, and M. Huang, "Bubble nucleation and gravitational waves from holography in the probe approximation," JHEP **07** (2023) 225, arXiv:2212.06591 [hep-ph].